Electrical Properties of Nanostructure Tin Oxide Thin Film Doped with Copper Prepared by Sol-Gel Method

M. A. Batal, G. Nashed, Fares Haj Jneed
Department of Physics, College of Science, University of Aleppo, Syria.

E-mail: fareshaj@gmail.com

(Received 28 April 2012, accepted 30 June 2012)

Abstract

Tin oxide thin film doped with copper were deposited on glass substrate, using co-deposition dip coating sol-gel technique, the films were doped with iron oxide at concentration (%5). Then it's sintered for 2 hour at temperature 600ºC.The electrical properties of the sample was studied by DC and AC measurements. From DC measurement, the shift of the quasi-Fermi E_F and the density of states at the Fermi level were determined. Electrical conductivity indicate the existence tow region I and II having different slop. Activation energy in I and II region were determined. From AC measurement, by drawing the relationship between complex part and real part of the complex impedance, we note that figures of the impedance spectrum have a semi-cycle which means that it is due to Debye model that involves the grain to be homogenous. Then the activation energy was determined by using AC and DC measurement. The density of free charge was determined as well as the density of trapped state determined too for the whole samples, too. By using Mott Schottky relationship we determined type semiconductor.

Keywords: Thin films, SnO_2, Impedance spectroscopy.

Resumen

La película delgada de óxido de estaño dopada con cobre donde es depositado el sustrato de vidrio, utilizando co-deposición de revestimiento por inmersión técnica sol-gel, las películas fueron dopadas con óxido de hierro a una concentración (%5). Entonces está sinterizado durante 2 horas a temperatura de 600°C. Las propiedades eléctricas de la muestra fueron estudiadas po0r las mediciones DC y AC. Desde la medición DC, el desplazamiento de la E_F cuasi-Fermi y la densidad de estados en el nivel Fermi fueron determinados. La conductividad eléctrica indica la existencia de remolque región I y II teniendo diferente decantación. La activación de energía en la región I y II fueron determinados. Desde la medición AC, mediante la elaboración de relación entre la parte compleja y la parte real de la impedancia compleja, notamos que las figuras del espectro de impedancia tienen un semi-ciclo lo que significa que se debe al modelo Debey que implica el grano para ser homogéneo. Entonces la activación de energía se determinó mediante el uso de las mediciones AC y DC. La densidad de carga libre fue bien determinada como la densidad de estado atrapado determinado también para todas las muestras, también. Mediante el uso de la relación Mott Schottky determinamos un tipo de semiconductor.

Palabras clave: Películas delgadas, SnO_2, espectroscopía de impedancia.

PACS: 85.40.Xx, 82.80.Dx **ISSN 1870-9095**

I. INTRODUCTION

Photo catalytic H2 production from water-splitting process using semiconductors and solar energy is believed to be one of the most promising renewable technologies [1]. Since pioneering work from Fujishima and Honda [2], many attempts to enhance the efficiency of water-splitting process using various semiconductors have been made at various laboratories [3, 4, 5]. Semiconductors with small and medium band gaps, show lower light-harvesting ability in visible light [6]. Therefore, coupling of semiconductors with different band gaps is good approach to prepare photo catalysts with high activity and good stability. The excited electrons can transfer in coupled semiconductors from the high conduction band to the low one, leading to efficient separation of photo generated electron-hole pairs.

The SnO2 exhibits good activity and stability under irradiation in both acidic and basic atmosphere. However, the pure SnO2 shows much lower photo catalytic activity even under UV irradiation due to its large band gap (3.6eV) [7]. To improve its photo catalytic activity, it is necessary to couple SnO2 with another semiconductor with lower band gap. The CuO is a p-type semiconductor with a small band gap (1.7-2.1eV). If the SnO2 is coupled with the CuO, the n-SnO2/p-CuO heterojunctions can be formed in. The photo generated electrons from SnO2 can easily migrate to

CuO. This favors the separation of photo generated electrons with holes, leading to enhancement of photo catalytic activity. The SnO_2 nanocomposites have been studied as gas sensor materials [8, 9, 10]. The performance of SnO_2/CuO nanocomposite, it's better to know more about the electrical properties of SnO_2/CuO. The objective of this study is to fabricate SnO2 doped with CuO photo catalyst, and to see when it's converted to P-type semiconductor. The SnO_2/CuO photo catalysts have been prepared by simple co-deposition using sol-gel method.

II. EXPERIMENTAL

The SnO_2/Cu thin films have been prepared by the simple co-deposition using Sol-Gel dip coating method. $SnCl_4.5H_2O$ and $CuCl_2.2H2O$ are used as starting materials. Typically, $SnCl_4$ and $CuCl_2$ with a desired weight ratio (Table I) are mixed together in Ethanol. The obtained solution is continuously stirred at 25ºC for 2h and aged 2 days. By using dip coating technique, thin films were deposited on glass substrate and cleaned by conventional method dried at 80ºC and sintered at 600ºC for 2h.

III. STRUCTURAL CHARACTERIZATION OF FILMS

X-ray diffraction (XRD) pattern of SnO_2 doped with Cu films was recorded by Philips system using Cu Kα (λ=0.154056nm) radiation with 2θ in the range 20-70º as Fig. (1-a).

From the (XRD) spectrum, the film is polycrystalline in nature having all peaks corresponding to the specific planes with maximum intensity peak from (110) planes. The relative intensity of all XRD peaks decreases in Cu^{+2}-doped film which can be attributed to incorporation of Cu^{+2} ions into the SnO_2 lattice and the resultant decrease of crystallite size. This is also evidenced by the increase in the full width at half maxima (FWHM) of the XRD peaks with increase in Cu^{+2} doping in the SnO_2 film. Furthermore, the fact that Cu^{+2} ion has smaller radius than Sn^{+4} ion, SnO_2 doping with Cu^{+2} should results in contraction of the lattice parameters. The average crystalline size was calculated using the Scherrer's formula based on the XRD patterns [11, 12, 13]:

$$D = k\lambda / (\delta w \cos\theta). \qquad (1)$$

Where: D is the size of granule, δw the wideness of peck opening at the middle of intensity, measured by Radian, k is constant (~1) wave length used by XRD λ: is the X-ray wavelength and its value (0.154nm), θ diffraction angle. Table I shows crystallite size of the films deposited on glass substrates.

Fig. (1-b) shows image SnO_2 doped with Cu with AFM device.

TABLE I. Summary of the XRD parameters and crystallite size mean grain size for different crystallographic of sample.

Crystallite Size (nm)			
Peak	110	101	211
SnO_2/Cu	26.57	41.25	59.47

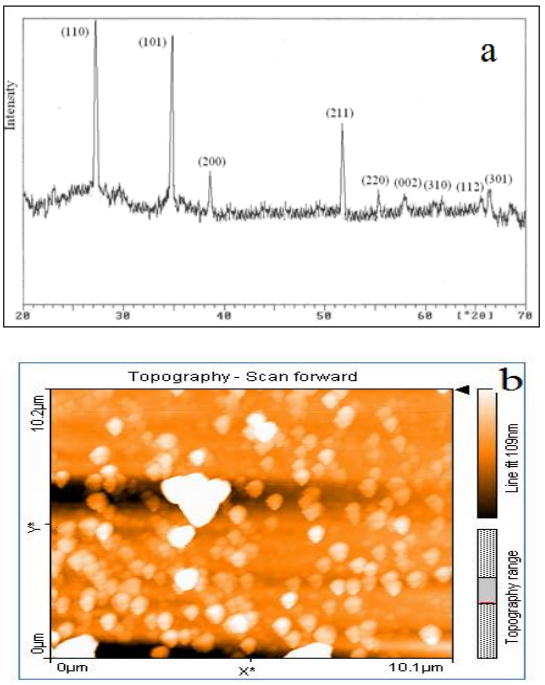

FIGURE 1. (a) XRD pattern SnO_2 doped with Cu (b) image with AFM of SnO_2 doped with Cu.

IV. (I-V) CHARACTERISTIC

DC measurements carried out using high resistance meter (hp 4339A). I-V characteristic were taken at constant temperature (150, 200, 250C) for all samples. Fig. (2) show the I-V characteristic. The *I–V* curves indicate two regions (I and II). At lower voltages (region I), the conduction is Ohmic, *i.e.* the current changes linearly with voltage, But, at higher voltages (region II), the conduction is the nonohmic. The slope of the second region II

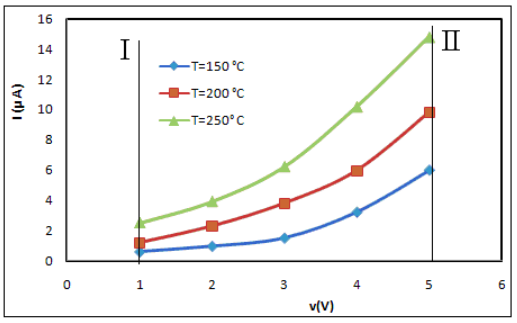

FIGURE 2. Current in function of applied voltage (a) T=150ºC, (b) T=200ºC, (c) T=250ºC.

decreases with increasing temperature. This confirms the presence of space charge limited conductivity, *i.e.*, high-electric conductivity region is governed by the injected space charge. The density of states at the Fermi level can be determined using the following relation [14]:

$$N(E_F) = \frac{2\varepsilon_r \varepsilon_0 \Delta V}{ed^2 \Delta E_F}. \quad (2)$$

Where

$$\Delta E_F = kT \ln \frac{I_2 V_1}{I_1 V_2}. \quad (3)$$

E_F is the shift of the quasi-Fermi level, ΔV is the change of applied voltage, e is the electronic charge, ε_r is the dielectric constant of the material (9.65 for SnO2) [14], d the film thickness and k is the Boltzmann constant. Using relation (2) and (3) the shift of the quasi-Fermi E_F and th 1e density of states at the Fermi level were determined. Table II gives Density of states at Fermi level.

TABLE II. Density of states at Fermi level.

$N(E_F)$ ($eV^{-1}m^{-3}$)	T=150ºC	T=200ºC	T=250ºC
SnO_2/CuO	2.6E+19	3.4E+19	8.7E+19

V. ACTIVATION ENERGY

The electrical conductivity dependence on temperature of the SnO2 film is shown two different regions having different slopes and it can be analyzed by the following relation:

$$\sigma = \sigma_0 \exp(-\frac{\Delta E}{kT}). \quad (4)$$

Fig. 3 shows the plot of $\ln \sigma$ in function of 1/T in Region I and region II for all samples.

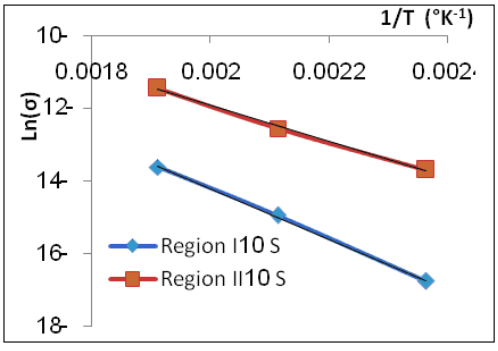

FIGURE 3. Plot of $\ln \sigma$ in function of 1/T.

Where ΔE is the activation energy, T is the temperature, k is the Boltzmann constant and σ_0 is the pre-exponential factor. The electrical conductivity of the film increases with the increase of temperature. The increase in electrical current and conductivity with temperature in the region I is lower than that of the increase in electrical conductivity in the region II. The ΔE value corresponds to the activation energy E_a of the donor or acceptor levels as the SnO2 is a n-type or p-type semiconductor. The E_a values for regions I and II were determined from the slopes of the linear regions of Fig. (1) and were, Table III gives ΔE at region I and region II for all samples found.

TABLE III. Activation energy for all samples at region I and II.

Sample	E_a(eV) at region I	E_a(eV) at region II
SnO_2/Cu	0.5107	0.3485

The activation energies are due to the presence of shallow and deep donor levels in the band gap of the SnO2 semiconductor. The activation energy value of region I of corresponds to the shallow donor level, while the activation energy value of corresponds to the deep donor level. These levels may result from ionized defects. The presence of two donor levels has been reported by Vishwakarma *et al.*, for CVD films. The increase in conductivity of the samples with temperature is due to decrease in grain boundary concentration and increase in ionized defects such as oxygen vacancies, which increase carrier concentration and mobility of the charge carriers [15-16]. Thus, it is evaluated that the existence of the two donor levels in SnO2 studied is due to the ionized defects such as oxygen vacancies.

VI. AC MEASUREMENTS

AC measurement carried out using GAIN PHASE ANALYZER (Schlumberger-SI1253). A complex impedance spectrum in frequency range (1-20000HZ) and at constant voltage (v=5V), and different temperature (150, 200 and 250) where taken for thin film.

$$Z(\omega) = R(\omega) + jX(\omega). \quad (5)$$

Figure (4) shows the relationship between the imaginary part X(ω) and the real part R(ω) of the complex impedance. We note that impedance spectrum has a semi-cycle which means that it's due to Debye model which involves the grain to be homogenous.

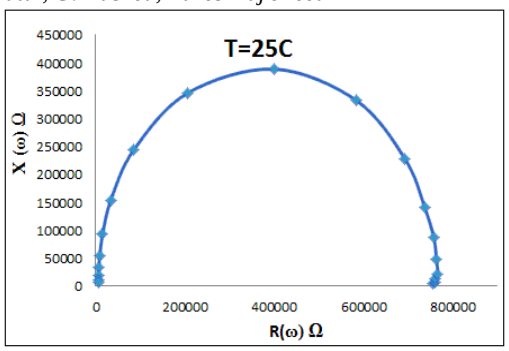

FIGURE 4. X(ω)=f[R(ω)].

To define The charge concentration and The change density of trapped state, complex impedance spectrum taken for all the film at temperature (150, 200, 250)˚C for sample as Fig. (5).

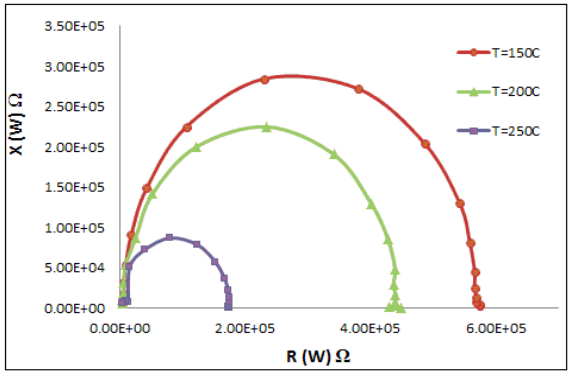

FIGURE 5. X(ω)=f[R(ω)]

From above figures, we note that when temperature of the samples rises, semi-cycle will be deformed and the shape of grain deformed, too. Debby model transfers to Cole-Cole model. To calculate the activation energy of prepared film, frequencies values had been taken at X(ω)=R(ω) from impedance spectrum at different temperature, where the following expression can be applied:

$$f = f_0 e^{-Ea/KT}. \qquad (6)$$

By taking Ln(f) as function of 1/T; activation energy can be determined. The charge concentration (elections or holes) were determined from the relation:

$$N_d = N_0 e^{\frac{-E_a}{2KT}}. \qquad (7)$$

The change density of trapped state calculated from the following expression [17]:

$$N_S = \left(\frac{2\varepsilon_0 \varepsilon_r N_d \Psi}{q} \right)^{1/2}. \qquad (8)$$

Table IV gives the values of different parameters for all samples.

TABLE IV.

T(ºC)	25	250
N_d/cm^3	3.11E20	5.59E20
N_s/cm	1.37E14	4.83E14

From Table IV, we note the biggest values of (N_d and N_S) are for thin film, and increase when temperature rises.

VII. INVERT FROM N-TYPE TO P-TYPE

By calculating the capacitance between grains boundary, then by applying the following Mott – Schottky expression [18]:

$$\left(\frac{1}{C} - \frac{1}{2C_0}\right)^2 = \frac{2}{e\varepsilon_0 \varepsilon_r (N_d - N_a)} (\Psi + V). \qquad (9)$$

Where C_p, C_0: are the parallel capacitance between the grain at v≠ 0 and v=0 respectively.

Figure (6) shows, the relation between $\left(\frac{1}{C} - \frac{1}{2C_0}\right)^2 = f(V)$ as function of applied voltage. When N_d >> N_a the slope will be positive and the semiconductor is n-type; when N_a >> N_d the slope will be negative and the semiconductor is p-type.

Table V gives different values of N_d or N_a and the type of carriers charge.

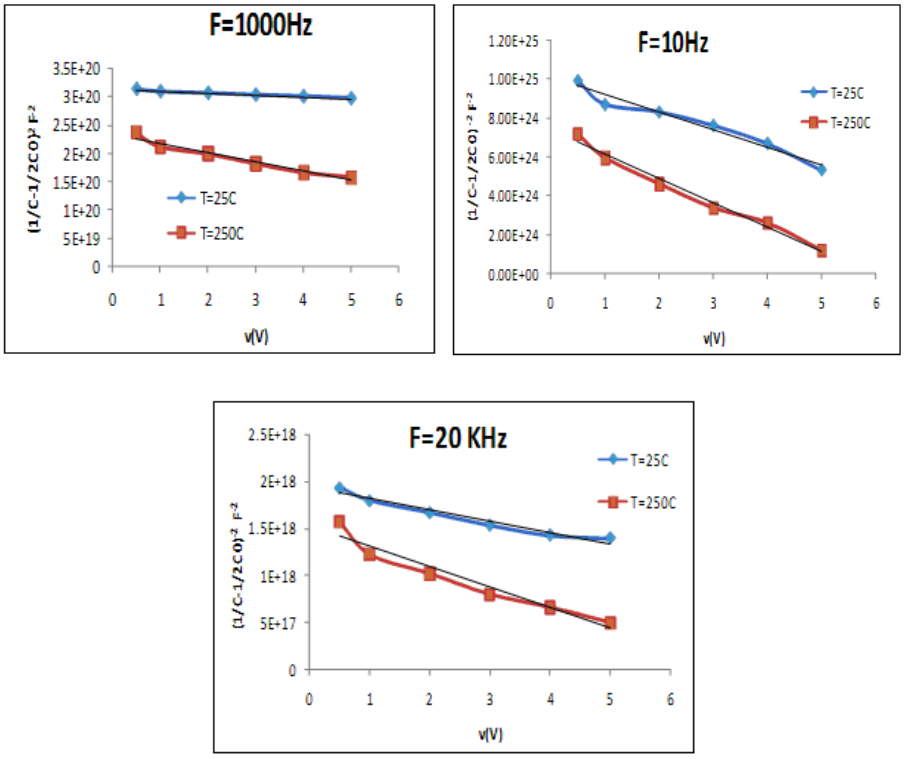

FIGURE 6. $(\frac{1}{C}-\frac{1}{2C_0})^2 = f(V)$.

Table V indicates the values of the density of shallow states (N_a or N_d) and the type of carrier of charges.

TABLE V.

F(Hz)	10	1000	20000
N_d or N_a/cm^3(T=25C)	2.32E16	5.8E21	1.93E23
N_d or N_a/cm^3(T=250C)	5.8E17	3.87E22	1.16E24
N_S /cm^3(T=25C)	3.45E12	1.72E15	9.95E15
N_S /cm^3(T=25C)	1.72E13	4.45E15	2.44E16
Semiconductor type	p	p	p

VIII. CONCLUSION

The increase in electrical current and conductivity with temperature in the region I is lower than that of the increase in electrical conductivity in the region II. The ΔE value corresponds to the activation energy E_a of the donor or acceptor levels as the SnO2 is a n-type or p-type semiconductor. The transition from n- to p-type conductivity on n-type semiconductor can be caused by a formation of an inversion layer at the surface and therefore to the inversion of the type of mobile carrier at the surface [19-20].visible light with different intensity cause a decrease in electrical resistance which release free charges, these free charge contribute to Photo catalytic H2 production.

REFERENCES

[1] John, N. A., *The multiple role for catalysis in the production of H2*, Appl. Catal. A. Gen. **176**, 159-176 (1996).

[2] Fujishima, A., Honda, K., *Electrochemical photolysis of water at a semiconductor electrode*, Nature **238**, 37-38 (1972).

[3] Sreethawong, T., Yoshikawa, S., *Enhanced photocatalytic hydrogen evolution over Pt supported on mesoporous TiO2 prepared by single-step solegel process with surfactant template*, Int. J. Hydrogen Energy **31**, 786-796 (2006).

[4] Zhang, Y. J., Yan, W., Wu, Y. P., Wang, Z. H., *Synthesis of TiO2 nanotubes coupled with CdS*

nanoparticles and production of hydrogen by photocatalytic water decomposition, Mater Lett. **62**, 3846-3848 (2008).
[5] Li, Y. X., Xie, C. F., Peng, S. Q., Lu, G. X., Li, S. B., *Eosin Y-sensitized nitrogen-doped TiO2 for efficient visible light photocatalytic hydrogen evolution*, J. Mol. Catal. A. Chem. **282**, 117-123 (2008).
[6] So, W. W., Kin, K. J., Moon, S. J., *Photo-production of hydrogen over CdSeTiO2 nanocomposite particulate films treated with TiCl4*, Int. J. Hydrogen Energy **29**, 229-234 (2004).
[7] Gurunathan, K., Marthamuthu, P., Sastri, M. V. C., *Photocatalytic hydrogen production by dye-sensitized Pt/SnO2 and Pt/SnO2/RuO2 in aqueous methyl viologen solution*, Int. J. Hydrogen Energy **22**, 57-60 (1997).
[8] A. Boudjemaaa, A., Boumazaa, S., Trarіc, M., Bouarabb, R., Bougueliac, A.*, *Physical and photo-electrochemical characterizations of a-Fe2O3. Application for hydrogen production*, International Journal o f Hydrogen Energy **34**, 4268-4274 (2009).
[9] Zhou, X. H., Cao, Q. X., Huang, H., Yang, P., Hu, Y., *Study on sensing mechanism of CuOeSnO2 gas sensors*, Mater Sci. Eng. **B 99**, 44-47 (2003).
[10] Pagnier, T., Boulova, M., Galerie, A., Gaskov, A., Lucazeau, G., *Reactivity of SnO2eCuO nanocrystalline materials with H2S: A coupled electrical and Raman spectroscopic study*, Sensor Actuator B Chem. **71**, 134-49 (2000).
[11] Junbo, W., Minge, Y., Yingmin, L., Licheng, C., Yan, Z., Bingjun, D., *] Junbo, W., Minge, Y., Yingmin, L., Licheng, C., Yan, Z., Bingjun, D., Synthesis of Fe-doped nanosized SnO powders by chemical co-precipitation method* , J. Non-Cryst Solids **351**, 228-232 (2005).
[12] Rani, S., Roy, S. C., Karar, N., Bhatnagar, M. C., *Structure, microstructure and photoluminescence properties of Fe doped SnO 2thin films*, Solid State Commun. **141**, 214-218 (2007).
[13] Fang, L. M., Zu, X. T., Li, Z. J., Zhu, S., Liu, C. M., Zhou, W. L. *et al.*, J Alloy Compd. **261**, 454-467 (2008).
[14] YAKUPHANOGLU, F., *Electrical conductivity, Seebeck coefficient and optical properties of SnO2 film deposited on ITO by dip coating*, Journal of Alloys and Compounds **470**, 55-59 (2009).
[15] Pagnier, T., Boulova, M., Galerie, A., Gaskov, A., Lucazeau, G., *Reactivity of SnO2eCuO nanocrystalline materials with H2S: A coupled electrical and Raman spectroscopic study*, Sensor Actuator B Chem 2000; 71:134e9.
[16] Hwang, I. S., Choi, J. K., Kim, S. J., Dong, K. Y., Kwon, J. H., Ju, B. K. *et al.*, *Enhanced H2S sensing characteristics of SnO2 nanowires functionalized with CuO*, Sensor Actuat B-Chem 2009; 142: 105e10.
[17] Bueno, P. R., Cassia-Santos, M. R., Leite, E. R., Longo, E., Bisquert, J., Garcia-Belmonte, G., Fabregat-Santiago, F., *Nature of the Schottky-type barrier of highly dense SnO2 systems displaying nonohmic behavior*, Journal of Applied Physics **88**, 6545-6548 (2000).
[18] Fernandez-Hevia, D., Frutos, J., Mott–Schottky, D. E., *Behavior of strongly pinned double Schottky barriers and characterization of ceramic varistors*, Journal of Applied Physics **92**, 2890-2898 (2002).
[19] Morrison, S. R., *The Chemical Physics of Surfaces*, 2th Ed. (Plenum Press, New York, 1990), pp. 61–63.
[20] Wolkenstein, T., *Electronic Processes on Semiconductor Surfaces During Chemisorption*, (Plenum Press, New York, 1991), pp. 138–142.